# Aging of Polyethylene Pipes Transporting Drinking Water Disinfected by Chlorine Dioxide. Part II—Lifetime Prediction

**Xavier Colin,[1] Ludmila Audouin,[1] Jacques Verdu,[1] Magali Rozental-Evesque,[2] Benjamin Rabaud,[2] Florencio Martin,[3] Francis Bourgine[4]**

[1] *Arts et Métiers ParisTech, LIM, 151 boulevard de l'Hôpital, 75013 Paris, France*

[2] *SUEZ-ENVIRONNEMENT, CIRSEE, 38 rue du président Wilson, 78230 Le Pecq, France*

[3] *VEOLIA-ENVIRONNEMENT, ANJOU RECHERCHE, Chemin de la Digue, B.P 76, 78603 Maisons Laffitte, France*

[4] *SAUR Direction Métiers, Les Cyclades, 1 rue Antoine Lavoisier, 78064 Saint-Quentin-en-Yvelines Cedex, France*

**This article deals with the failure of polyethylene pipes transporting chlorine dioxide (DOC) disinfected water under pressures of few bars. Accelerated aging tries made at 20 or 40°C show that the antioxidant is rapidly consumed in a superficial layer until a depth of about 1.2 mm. Carbonyl groups appear in a sharper layer of few hundreds micrometers. Natural aging results at various places, for various times up to about 30 years, reveal also a superficial attack with a depth of the order of 1.2 mm. An antioxidant loss by migration, in the whole sample thickness, is also observable. The shape of antioxidant concentration profiles indicates that the crossing of interfaces controls partially the whole migration kinetics. Failures, with brittle cracking, were observed in natural aging, after exposure times of the order of 5–15 years, i.e., far before the expected lifetime (50 years). A kinetic model has been elaborated to predict the time to failure. It is based on a chemical unit, which models the radical processes induced by DOC, and a mechanical unit based on an empirical creep law and a failure criterion depending of the molar mass calculated by the chemical unit.** **POLYM. ENG. SCI., 49:1642–1652, 2009.** 

## INTRODUCTION

This article deals with the effect of chlorine dioxide (DOC) on aging of polyethylene (PE) pipes for the transport of drinking water under pressure. In the first part of this article [1], it has been shown that DOC, which is a free radical, is able to initiate radical chain oxidation in PE. Oxidation induces random chain scission and this latter leads to embrittlement when the weight average molar mass $M_W$ becomes typically lower than 70 kg mol$^{-1}$. A mechanistic scheme, based on previously established one for low-temperature PE thermo-oxidation [2, 3] incorporating DOC reactions, has been built [1]. In the chosen accelerated aging conditions, (high-DOC concentrations), the role of antioxidants was considered negligible owing to their very high-reactivity with DOC and the low sample thickness favoring DOC diffusion. The case of pipe natural aging is, indeed, more complex, first because DOC concentrations are 100–1000 times lower (typically 0.1–0.2 ppm in drinking water), second because pipe degradation is presumably diffusion controlled, owing to the relatively high wall thickness (few millimeters). Then, kinetic modeling needs to take into account antioxidant reactions, and the diffusion of molecular reactive species: oxygen, antioxidant, and DOC.

The first objective of this work is to complete the kinetic model presented in the first part of this article [1], incorporating the above factors. The primary function of this model is to predict the change of molar mass in the superficial layer at the polymer/water interface, because it is the direct cause of premature crack initiation. The model allows to predict many other chemical quantities among which two are especially interesting: the depth profile of carbonyl groups concentration and the depth profile of stabilizer concentration. As a matter of fact, both profiles are experimentally checkable from routine methods and offer thus two especially pertinent ways for

*Correspondence to*: X. Colin; e-mail: xavier.colin@paris.ensam.fr
DOI 10.1002/pen.21387
Published online in Wiley InterScience (www.interscience.wiley.com).

the model validation. At this state, the model would be able, in principle, to predict the pipe embrittlement in its superficial layer in contact with disinfected water, i.e., the time at which this latter would loose its ability to sustain plastic deformations [4]. But for users, what is important is to predict the time to failure under pressure.

The second objective of this work is to explore a semi-empirical way to model the "chemical–mechanical coupling" responsible for pipe fracture in use conditions. In practice, lifetime prediction of pipes under pressure is based on two principles [5–7]:

"Regression" plots: Log(hoop stress $\sigma$) = $f$[Log(time to failure $t_F$)] are linear in certain stress-time intervals.

The temperature dependence of $t_F$ can be represented by Arrhenius law. In other words, it is possible to construct a regression master plot using adequate Arrhenius shift factors [5].

In isothermal plots, one, two, or three kinetic regimes of fracture can be observed, depending on the observation time, polymer structure, or environment reactivity, as schematized in Fig. 1 [6]. In the absence of chemical degradation (no change of molar mass distribution), two regimes: I and II (or eventually only one: I in cross-linked PE pipes [8] and perhaps in the last linear PE generation PE100) can be observed. It is usual to consider that regime I corresponds to ductile failure although, at least in cross-linked PE pipes, brittle failure can also occur in regime I at low-stress values [8]. This regime is characterized by a low-slope: $\Delta(\text{Log } \sigma)/\Delta(\text{Log } t_F) \sim 0.03$. Regime II corresponds always to brittle regime. Here, $\Delta(\text{Log } \sigma)/\Delta(\text{Log } t_F) \sim 0.3$. The dashed arrow in Fig. 1a indicates the sense of variation of the transition time $t_C$ from one PE generation to the next one. The same figure indicates the range of the use hoop stresses (typically less than 1 MPa). The minimum lifetime ($t_m$ in Fig. 1a) is expected to be about 50 years. Regime III corresponds to chemical ageing. The corresponding straight line is almost vertical: the incertitude on the determination of its parameters is thus very high. Regime III can totally supplant regime II (Fig. 1c) when the environment is especially reactive. This is the case, apparently, of certain portions of the DOC disinfected water network which failed after a few years exposure, in the south of France, especially in the dog-days of 2003. The regression analysis is not well adapted, to our opinion, to lifetime prediction in regime III, at least because each regression graph corresponds only to one environment composition and because physical and chemical failures do not necessary obey to the same time-temperature superposition principles, that complicates seriously the analysis. It seemed to us interesting to develop a new kinetic model based on the following principles:

It must predict failure in function of the following parameters: PE initial $M_W$ value, cristallinity ratio, antioxidant nature, and concentration, temperature, water pressure, DOC concentration.

It must be designed to work as well in isothermal as in anisothermal conditions (to take into account seasonal temperature variations).

It must predict fracture as well in regime II as in regime III (regime I is ignored owing to its low-practical interest).

It must predict experimentally accessible characteristics, for instance carbonyl and stabilizer concentration profiles, molar mass in the superficial layer, grafted chlorine content, to permit its validation.

## EXPERIMENTAL

### *Materials*

All the samples under study were black polyethylene pipes for the transport of drinking water, obeying the French standard: NF EN 12201. They had the following features: 2.0–2.5% by weight of carbon black; a melting point: $T_m$ = 120–130°C; a crystallinity ratio: $X_C$ = 35–50%; a weight average molar mass: $M_W$ = 100–150 kg mol$^{-1}$; an oxidation induction time at 190°C: $t_i$ = 155–180 min. The pipe diameters ranged between 30 and 63 mm, the pipe wall thickness was between 3.0 and 7.0 mm.

Pipe sections having ages ranging from 1 to 30 years were taken in the drinking water network in various places of the south of France. All the samples except two were taken in network parts where chlorine dioxide (DOC) was used as disinfectant. Two samples were taken in a network part, in Alp Mountains, where no disinfectant was used. About 130 samples, taken in more than 50 distinct places, were studied. Certain samples displayed open brittle cracks, others displayed no visible damage.

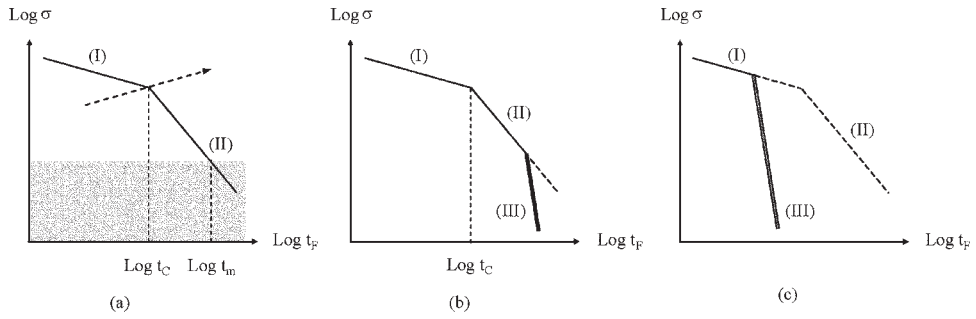


FIG. 1. Shape of usual regression curves.

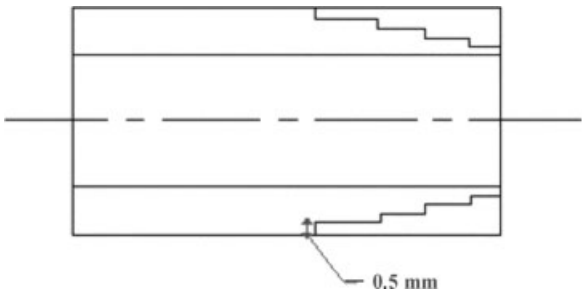


FIG. 2. Schematization of pipe machining to obtain ~0.5 mm-thick slabs.

A pipe of 40 mm diameter, 4.5 mm wall thickness, named sample A in the following, was chosen for accelerated aging tests. It displayed the following initial characteristics: 2.5% by weight of carbon black; a melting point: $T_m = 130°C$; a crystallinity ratio: $X_C = 45\%$; a weight average molar mass: $M_W = 350$ kg mol$^{-1}$; and an oxidation induction time at 190°C: $t_i = 165$ min. It is stabilized by a classical antioxidant mixture: 0.1% by weight of Irganox 1010 plus 0.05% by weight of Irgafos 168. The presence of secondary antioxidant of the phosphite-type was confirmed by elemental analysis.

### *Accelerated Aging*

A pipe section of ~100 cm length was placed on a thermostated loop in which a controlled DOC solution was put in circulation at 20 or 40°C at atmospheric pressure. DOC was periodically titrated and its concentration readjusted at its initial value. DOC solutions were produced by reaction of chlorite anion with chlorhydric acid in stoichiometric excess. The global reaction can be summarized as follows:

$$5\,NaClO_2 + 4\,HCl \rightarrow 4\,ClO_2 + 5\,NaCl + 2\,H_2O$$

The excess of chlorhydric acid increases the reaction yield.

DOC concentrations ranging from 1 to 100 ppm were studied. The pipe samples were exposed up to 20 weeks. Preliminary tests showed that aging characteristics are almost independent of the PE origin, the water pH, and the scaling character of water.

### *Carbonyl and Antioxidant Thickness Profiles*

Pipes were machined and slabs of 0.5 mm thick were taken at various depths according to the scheme of Fig. 2. The slabs were analyzed by IR spectrophotometry in Attenuated Total Reflectance mode, essentially to record the carbonyl peak at ~1720 cm$^{-1}$.

Samples of 5–10 mg, taken in slabs, were analyzed by DSC to determine the oxidation induction time (OIT) at 190°C in an oxygen flow of 50 mL min$^{-1}$. It will be considered that OIT changes are essentially due to the phenolic antioxidant consumption, for the following reasons:

Control samples made of "pure" PE with the same antioxidant, in the same concentration, as in sample A, were prepared and their OIT was determined. Its value: 158 min is very closed to the one of sample A, showing that carbon black plays a negligible stabilizing role in the conditions under study.

As it will be shown, the induction period vanishes totally after aging, in the superficial layer where DOC penetrates, whereas there is no sign of carbon black destruction.

Phosphite costabilizers are known to act essentially through ionic processes [9] and to work essentially at high-temperature, in processing conditions.

According to the above hypotheses, if $[AH]_0$ and $[AH]$ are the phenol concentration values, respectively, before exposure and after an exposure of duration $t$ where the induction time, initially $t_{i0}$, has decreased to a value $t_i$, one would have [10, 11] the following:

$$\frac{t_i}{t_{i0}} = \frac{[AH]}{[AH]_0} \tag{1}$$

## RESULTS

### *Induction Time Profiles After Accelerated Aging*

Some induction time profiles obtained at 40°C for various exposure times and DOC concentrations are shown in Fig. 3. The antioxidant consumption in a superficial layer increases with time for a given DOC concentration and with DOC concentration for a given exposure time. The "front" of DOC attack is almost vertical. It tends toward a pseudo-asymptotic depth of the order of 1.2 mm when exposure time increases. The stabilizer concentration remains unchanged, within experimental incertitudes, in the core of the pipe wall. No antioxidant consumption was observed when pipe samples were exposed in DOC free water in the same exposure conditions.

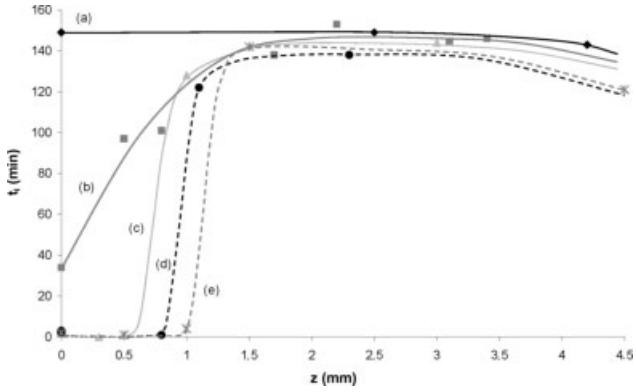


FIG. 3. Oxidation induction time profiles after exposure at 40°C in solutions with different DOC concentrations as follows: (a) after 99 days in dematerialized water; (b) after 2 days in 5 ppm; (c) after 10 days in 31.8 ppm; (d) after 51 days in 66.8 ppm; (e) after 99 days in 68.5 ppm.

 DOI 10.1002/pen

*Carbonyl Profiles After Accelerated Aging*

A carbonyl profile obtained after 99 days of exposure in a 66.5 ppm DOC solution at 40°C is shown in Fig. 4, where it is superimposed to the corresponding induction time profile. Carbonyls appear in a superficial layer of few hundreds micrometers, thinner than the antioxidant consumption layer. As shown in the first part of this article [1], DOC induces PE oxidation but, here, this latter is diffusion controlled.

*Induction Time Profiles After Natural Aging*

Some characteristic induction profiles are presented in Fig. 5. These results call for the following comments:

Comparison between disinfected and non disinfected water shows that the superficial antioxidant consumption near the inner pipe surface is clearly due to DOC attack.

The depth of the "antioxidant consumption layer" is not very different from one location or one age, to another. It is also close to the one observed after accelerated aging, i.e., of the order of 1.2 mm.

Contrarily to the case of accelerated aging, the induction time decreases in the core of the pipe wall, as a result of antioxidant physical loss. The induction time in the middle of the wall $t_i$ ($L/2$) has been plotted against exposure time in Fig. 6. Except for some cases of anomalously short lifetime, the points are located between two boundaries corresponding to characteristic times between about 10 and 20 years, the characteristic time being defined as the time to reach an induction time value of about 50 min. There is no difference, from this criterion, between DOC disinfected and nondisinfected water, showing that the antioxidant concentration decrease in the middle of the wall is effectively due to physical migration.

In the outer wall half, the profile remains almost horizontal. This is not the case at high-temperature (~100°C) aging, where the antioxidant concentration is maximum near the middle of the wall and zero at the outer surface [7, 11–13]. The observed profile indicates that, in natural aging conditions, i.e., close to ambient temperature, the antioxidant loss is, at least partly, governed by its evaporation rate.

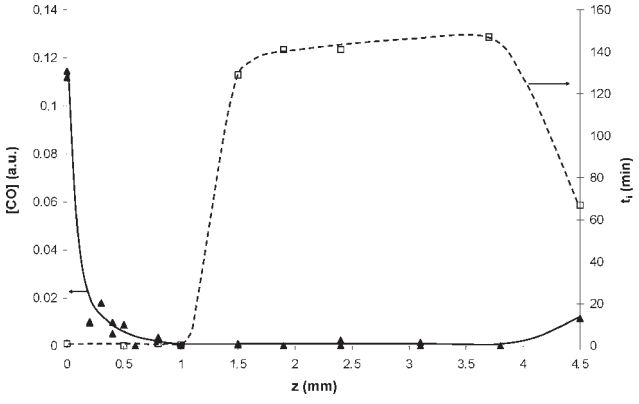


FIG. 4. Profiles of carbonyl groups (▲) and oxidation induction time (□) after 99 days of exposure in a 66.5 ppm DOC solution at 40°C.

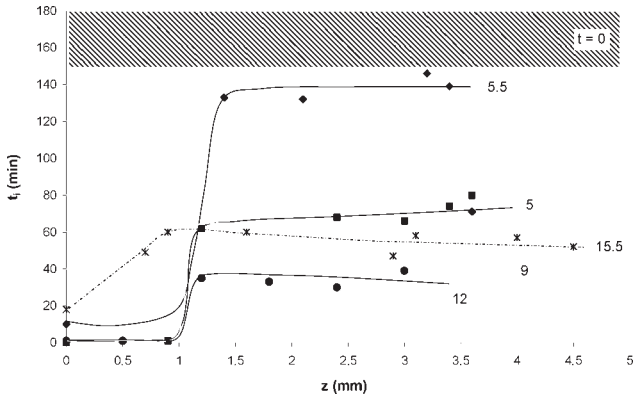


FIG. 5. Typical oxidation induction time profiles after natural aging. The numbers in the figure indicate the pipe age in years. All the pipes have been used with DOC disinfected water except one used with non-disinfected water (dashed line).

*Time to Failure in Natural Aging*

For about two dozens of samples, the exposure conditions (pressure, temperature) and the time to failure were known with a reasonable approximation. The results have been put in a regression plot ($\log(\sigma) = f[\log(t_F)]$), in Fig. 7 where Brown and Lu data [5], corrected for a temperature of 15°C, were added. The times to failure are at least one order of magnitude lower than the ones predicted from regression analysis in the case of disinfectant free water.

## KINETIC MODEL

The aim of the kinetic model is to predict the time to failure $t_F$. It is based on the following principles:

Fracture is due to the polymer creep. The extent of this latter is characterized by an undefined parameter $\varepsilon$ which could be the overall strain, the anelastic strain, the local

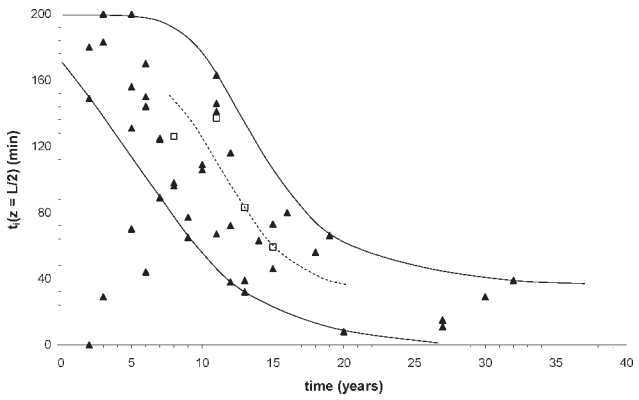


FIG. 6. Oxidation induction time in the middle of the wall ($z = L/2$) against exposure time for natural aging in DOC disinfected water (▲) and nondisinfected water (□) for pipes used in the south of France in the 1970–2005 period.

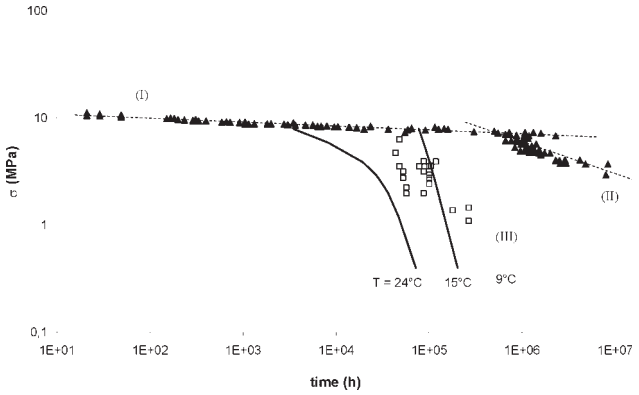


FIG. 7. $\mathrm{Log}(\sigma) = f[\mathrm{Log}(t_F)]$ curve determined from results reported by Brown and Lu [5] for a PE pipe containing pressurized water at 15°C (▲). Failure characteristics of pipes used in the south of France in the presence of DOC disinfectant in the 1970–2005 period have been superimposed (□). The model simulation of regime III (brittle regime in the presence of chemical degradation) at 15°C is represented by a continuous line. As an example, simulations made at 9 and 24°C are also given.

strain at a pertinent scale, for instance in the amorphous, interlamellar layer, etc ... The creep rate is supposed temperature- and time-dependent but aging independent. Its variation will be expressed empirically as follows:

$$\dot{\varepsilon} = k e_T \sigma t^{-a} \tag{2}$$

where $k$ is a constant, $e_T$ an Arrhenius factor: $e_T = \exp -\frac{H}{RT}$ and a an exponent expressing the self-retarded character of the polymer creep. $\sigma$ is the hoop stress.

The "creep extent" is thus given by the following:

$$\varepsilon = \int_0^t \dot{\varepsilon}\, dt = \frac{1}{1-a} k e_T \sigma t^{1-a} \tag{3}$$

In regime II, fracture occurs at constant "creep extent" $\varepsilon_F$. The value of $\varepsilon_F$ is assumed to be characteristic of a PE family characterized by a given type of morphology with close values of lamellar dimensions. Samples significantly different from the point of view of morphology, for instance copolymers of very different compositions, are expected to have distinct parameters values. *Equation 3* can be rewritten as follows:

$$\sigma = (1-a)\frac{\varepsilon_F}{k e_T} t_F^{-(1-a)} \tag{4}$$

This equation is identical to the one of "regression" straight line:

$$\mathrm{Log}\sigma = \mathrm{Log}\sigma_0 - a' \mathrm{Log} t_F \tag{5}$$

provided that:

$$a' = 1 - a$$

and

$$\mathrm{Log}\sigma_0 = \mathrm{Log}\left[\frac{\varepsilon_F}{k}\frac{(1-a)}{e_T}\right]$$

Thus, our "mechanical model" contains not less, not more information than "regression" straight lines. Indeed, the parameter values must be adjusted to agree with "regression" data on pipes tested in the absence of chemical degradation. $\varepsilon_F$ depends on the polymer molar mass and thus, decreases with the conversion of the chemical degradation process. The fracture process is schematized by Fig. 8.

According to the above hypotheses, the effect of aging on regression plots could be schematized by Fig. 9. Only regime (II) is considered. According to our hypothesis, creep kinetics is not modified by chemical aging, but the "creep extent" at rupture $\varepsilon_F$ decreases. This means that, if (IIu) corresponds to the regression straight line of the undegraded polymer, it is translated toward short times in (IIt) after a certain aging time. For a hoop stress $\sigma$, fracture will occur at the point A of abscissa $t_{F1}$. Let us now consider a try made at the hoop stress $\sigma - \Delta\sigma$. If degradation was stopped at time $t_{F1}$, then fracture would occur at point A′ of abscissa $t_{F2}$. However, degradation continues at times longer than $t_{F1}$ so that the regression straight line is again shifted toward short times. Then, fracture occurs in point B of abscissa $t_{F3}$ when it crosses the horizontal straight line of ordinate $\sigma - \Delta\sigma$.

There is basically no reason to suppose that the envelope of fracture points, passing by A and B, would be a straight line, however, since it is quasi vertical, it will practically appear as a straight line (regime III).

The link between this mechanical model and a chemical kinetic model can be established on the basis of the follow-

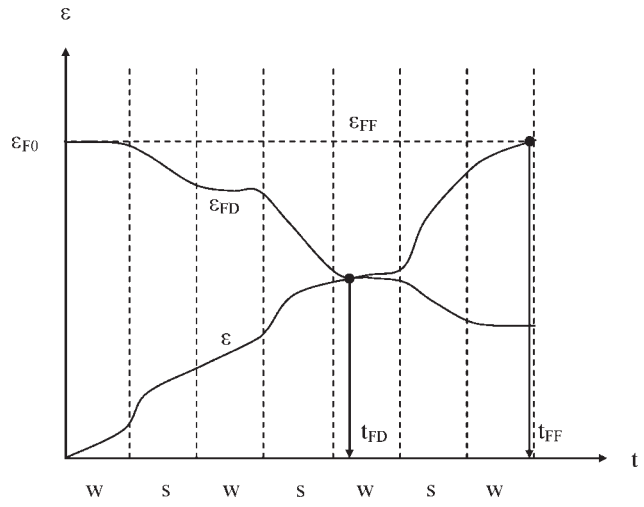


FIG. 8. Schematization of the changes of "creep extent" $\varepsilon$ and its critical value $\varepsilon_F$ with time under pressure. The slope changes could be due for instance to seasonal temperature variations (w: winter, s: summer). $\varepsilon_{FF}$ and $t_{FF}$ correspond to exposure in the absence of disinfectant. The corresponding value $t_{FF}$ is available in literature for isothermal tests. $\varepsilon_{FD}$ and $t_{FD}$ correspond to exposure in the presence of disinfectant.

 DOI 10.1002/pen

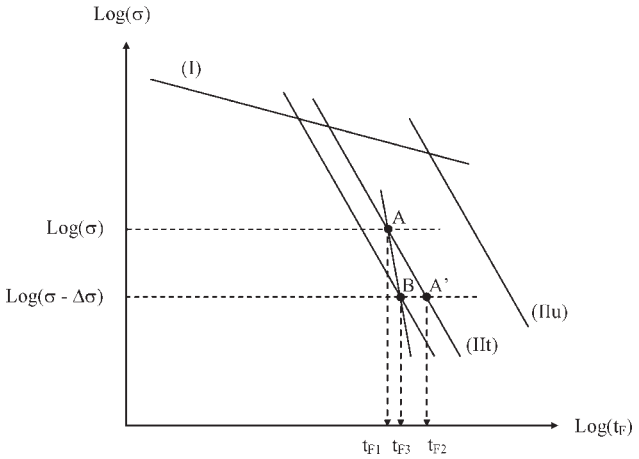


FIG. 9. Regression plot showing the effect of aging (see text).

ing considerations: The decrease of $\varepsilon_F$, i.e., the shift of the regime II straight line, is linked to the molar mass decrease. Various physical interpretations are available in the literature, for instance: chain disentanglement in the amorphous phase [14], destruction of tie-macromolecules [15–17], or rupture of craze fibrils [6]. It will be assumed that, whatever the true mechanism, the molecular weight dependence of fracture time can be approximated by a power law:

$$t_F \propto M_W^{\alpha} \tag{6}$$

that can be justified from the kinetic analysis of chain reptation [18].

Incorporating this law to the prefactor of *Eq. 4*, this leads to the following:

$$\mathrm{Log}t_F = A_0 + \frac{H}{2.3RT}(1+m) + \alpha m\,\mathrm{Log}M_W - \frac{1}{1-a}\mathrm{Log}\sigma \tag{7}$$

where $A_0$ contains all the prefactors.

$\alpha$ could be in principle determined on experiments in pipes differing by their molar mass distribution in the absence of chemical degradation. In a first approach, we will use the well-known rheological exponent as follows:

$$\alpha = 3.4$$

All the other parameters can be in principle determined from available experimental data, for instance Brown's regression plots [5]. The values used in the chosen example of lifetime prediction for an isothermal exposure at 15°C are given in Table 1.

A chemical kinetic model aimed to predict the local (at a given distance $z$ of the polymer/water interface) value of $M_W$ has been presented in Part 1 of this article. However, as it will be shown below, degradation is diffusion controlled, that leads to the existence of molar mass thickness gradients. These latter can be taken into account, in the mechanical model, as follows:

TABLE 1. Values of the kinetic parameters used for lifetime prediction 15°C.

| Kinetic parameter | Value |
|---|---|
| $A_0$ | −29.7 |
| $\frac{H}{2.3RT}(1+m)$ | 30.2 |
| $\alpha m$ | 3.2 |
| $\frac{1}{1-a}$ | 3.3 |

One expects that cracks initiate and propagate easily in the degraded superficial zone where the weight average molar mass is typically $M_W \leq 70$ kg mol$^{-1}$ [19].

According to the basic principle of fracture mechanics, pipe fracture can occur if the "primary cracks" have a length higher than a certain critical value $l_C$ [20]. Previous investigations seem to show that for PE, $l_C$ could be of the order of 100 $\mu$m [21]. It is thus proposed to take the $M_W$ value at a 100 $\mu$m depth to use in *Eq. 7*. This value (as the whole $M_W$ thickness profile) can be predicted from the coupled diffusion-reaction model (see below).

Diffusion-reaction coupling is incorporated into the chemical kinetic model as follows:

Three reactive molecular species susceptible of migrate through the pipe wall are considered: oxygen, phenolic antioxidant, and DOC. Each one is characterized by its diffusion coefficient $D_{O2}$ for $O_2$, $D_{AH}$ for the antioxidant, and $D_{DOC}$ for DOC. A Fickian term: $D_Y \frac{\partial^2[Y]}{\partial z^2}$ is added to each differential equation expressing the concentration changes of the species under consideration, and the whole system of differential equations is solved in each elementary layer dz keeping a local diffusion-reaction coupling and using a semi-implicit Rosenbrock's algorithm [22]. The resulting differential equations are reported in Appendix. Literature values are used for $D_{O2}$ [23] and for $D_{AH}$ [24]. $D_{DOC}$ is obtained using experimental results of accelerated aging tries (see below), using an inverse method [25]. Its Arrhenius parameters and its value at 15°C are given in Table 2.

For stabilizer transport, interface crossing is a partially rate controlling process, that leads to consider the following boundary conditions [26, 27]:

TABLE 2. Arrhenius parameters and values at 15°C of kinetic parameters (rate constants and coefficients of diffusion and stabilizer extraction/evaporation) for kinetic modeling.

| Kinetic parameter | Pre-exponential factor (L mol$^{-1}$ s$^{-1}$, m$^2$ s$^{-1}$, or s$^{-1}$) | Activation energy (kJ mol$^{-1}$) | Value at 15°C |
|---|---|---|---|
| $k_{1S}$ | $5.0 \times 10^{-2}$ | 0 | $5.0 \times 10^{-2}$ |
| $k_{S1}$ | $1.3 \times 10^{9}$ | 49.9 | 1.1 |
| $D_{O2}$ | $4.3 \times 10^{-5}$ | 35 | $1.9 \times 10^{-11}$ |
| $D_{DOC}$ | $2.0 \times 10^{-11}$ | 0 | $2.0 \times 10^{-11}$ |
| $D_{AH}$ | $9.1 \times 10^{4}$ | 115.7 | $9.7 \times 10^{-17}$ |
| $\beta_{AH0}$ | $1.9 \times 10^{-9}$ | 0 | $1.9 \times 10^{-9}$ |
| $\beta_{AHL}$ | $1.0 \times 10^{-10}$ | 0 | $1.0 \times 10^{-10}$ |

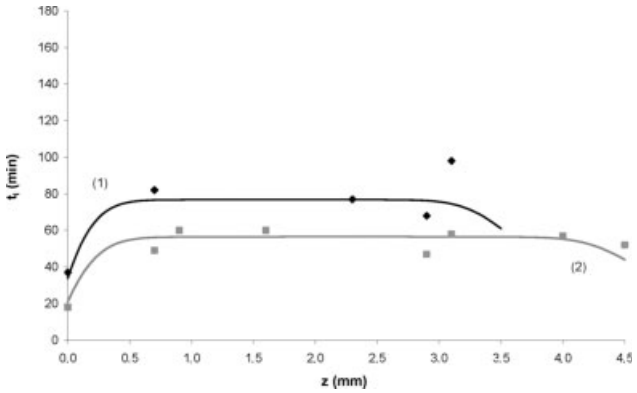


FIG. 10. Simulations of oxidation induction time profiles after exposure at 15°C in water free of disinfectant during 13 and 15.5 years. Theoretical data (the lines) and the experimental data (the points).

At the inner pipe surface/water interface $z = 0$ (extraction):

$$D_{AH}\frac{\partial^2[AH]_{z=0}}{\partial z^2} = -\beta_0[AH]_{z=0} \quad (8)$$

At the outer pipe surface/air interface $z = L$ (evaporation):

$$D_{AH}\frac{\partial^2[AH]_{z=L}}{\partial z^2} = -\beta_L[AH]_{z=L} \quad (9)$$

where $\beta_0$ and $\beta_L$ are coefficients of, respectively, water extraction evaporation.

They will be determined, here, from experimental antioxidant profiles obtained in the case of disinfectant free water (Fig. 10).

The input parameters are thus the following ones:

Water parameters: temperature, pressure, DOC concentration;

PE parameters: cristallinity ratio $X_C$, initial weight average molar mass $M_{W0}$, initial antioxidant concentration $[AH]_0$, antioxidant functionality $n_{AH}$, transport parameters of antioxidant: $D_{AH}$, $\beta_0$, and $\beta_L$;

Pipe parameters: diameter $d$ and wall thickness $L$.

The output quantities are as follows: All the quantities involved in the model, the most important one being the weight average molar mass in a subcutaneous layer: $M_W(z = 100\ \mu m)$.

The experimentally checkable quantities, i.e., antioxidant and carbonyl profiles are especially interesting because they allow, at least partially, the model validation.

## EXAMPLES OF SIMULATION

All the simulations have been made for a polyethylene sample of initial average molar mass $M_{n0} = 75$ kg mol$^{-1}$ and $M_{W0} = 150$ kg mol$^{-1}$. The phenolic antioxidant is the widely used Irganox 1010 of which the functionality is $n_{AH} = 4$. Its concentration was taken equal to the equilibrium concentration at 15°C: $[AH]_0 = 1.8 \times 10^{-3}$ mol L$^{-1}$ [24]. For the diffusion coefficient, a literature value: $D_{AH} = 9.7\ 10^{-17}$ m$^2$ s$^{-1}$ [24] was used. Interface exchange coefficients $\beta_0$ and $\beta_L$ were determined from the stabilizer concentration profiles of samples aged for 13 and 15.5 years in disinfectant free water (Fig. 10). Their Arrhenius parameters and their values at 15°C are given in Table 2.

In the case of accelerated aging, experimentally determined DOC concentrations and temperatures were used to simulate antioxidant concentration profiles (Fig. 3) and carbonyl profiles (Fig. 4). In these cases, since no pressure is applied, no fracture is observed, even at relatively high-degradation degrees of the wall superficial layer. A simulation of the antioxidant concentration profiles is shown in Fig. 11 where they can be compared with experimental ones. In the case of natural aging, simulations were made for pipe wall thicknesses varying from 3.0 to 4.5 mm. Some simulated profiles can be compared with experimental ones in Fig. 12. Small variations of the DOC concentration can exist from one place to another, calculations were made for a concentration of 0.15 ppm, which can be considered as a reasonable average value according to water suppliers. Simulations were made for two extreme temperatures: 9 and 24°C and for a medium temperature 15°C, which is probably close to the average temperature in most cases. The corresponding curves $\text{Log}(\sigma) = f[\text{Log}(t_F)]$ are plotted in the regression graph of Fig. 7. It can be observed that all the experimental points are located between both extreme curves and are close to the average one.

## DISCUSSION

Let us first consider the secondary functions of the model, i.e., mainly stabilizer and carbonyl thickness profiles. Their prediction is interesting first because they can

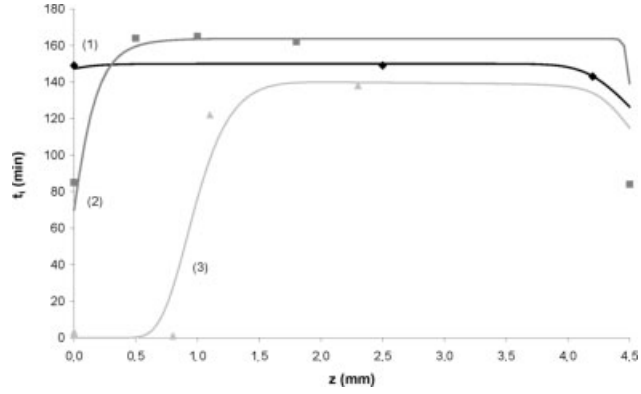


FIG. 11. Simulations of oxidation induction time profiles after exposure at 40°C in solutions with different DOC concentrations as follows: (1) after 99 days in demineralized water; (2) after 23 h in 10.1 ppm; and (3) after 51 days in 66.8 ppm. Comparison between theoretical profiles (the lines) and the experimental data (the points).

 DOI 10.1002/pen

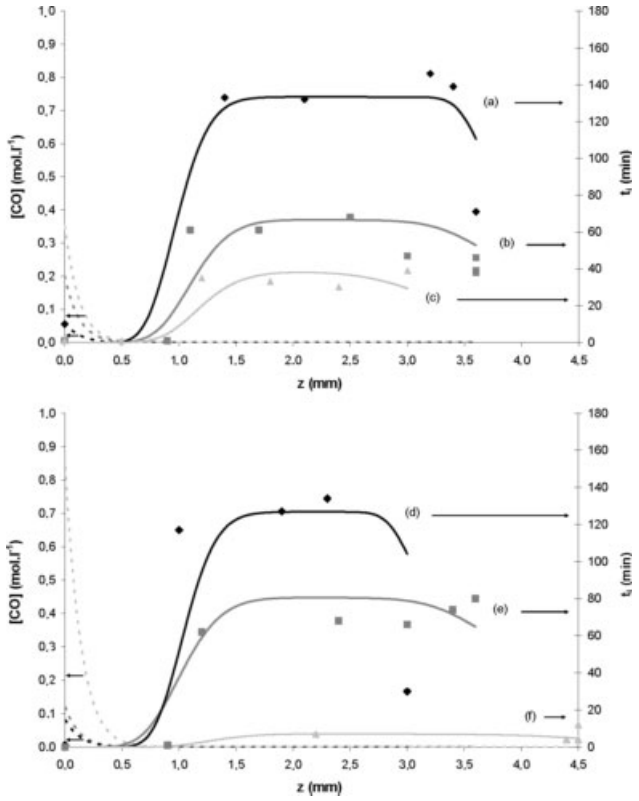


FIG. 12. Simulations of profiles of carbonyl group concentration and oxidation induction time after natural aging: (a) after 5.5 years at 13°C; (b) after 9 years at 19.5°C; (c) after 12 years at 19.5°C; (d) after 8 years at 11°C; (e) after 5 years at 24°C; and (f) after 18 years at 19°C. Comparison between theoretical profiles (the lines) and the experimental data (the points).

be considered as good validation criteria for the chemical kinetic model.

Let us first consider antioxidant profiles in the case of accelerated aging. Their most striking features are, no doubt, the abrupt shape of the DOC "penetration front" and the fact that the location of this latter tends toward a quasi asymptotic depth $z_\infty$ of the order of 1.2 mm at long exposure times. Both characteristics are well predicted by the model. The apparent stabilization of the DOC "penetration front" would be difficult to explain only with the DOC-antioxidant reaction. As a matter of fact, when the antioxidant has totally disappeared in a superficial layer, there is no obstacle to DOC penetration in deeper zones. The simplest explanation is that DOC penetration is controlled by its reaction with PE. This reaction is considerably slower than the DOC-antioxidant reaction:

$$\frac{k_{1S}}{k_{1d}} \approx 1.9 \times 10^3 \tag{10}$$

About the same reactivity ratio was found for $PO_2^\bullet$ radicals:

$$\frac{k_{S1}}{k_3} \approx 1.2 \times 10^3 \tag{11}$$

The antioxidant appears thus 1500 times more reactive than PE with moderately reactive radicals, that explains why antioxidant is rapidly destroyed by DOC.

Let us now consider antioxidant profiles in the case of natural aging. Their most striking features are as follows:

The existence of a quasi asymptotic depth of DOC penetration, practically the same (≈1.2 mm) as in accelerated aging.

The fact that the concentration profile displays an horizontal plateau in the middle and outer wall parts, of which the height decreases with exposure duration. It is clear that antioxidant migration is negligible in the timescale of accelerated aging tests (less than 1 year), but becomes noticeable in the case of exposure durations of several years. Almost all the stabilizer has disappeared, in most cases, after 20 years approximately.

The flatness of the plateau in the middle and outer parts of the wall brings interesting information: It indicates that the interface exchange at both sides of the wall controls practically the antioxidant transport kinetics, otherwise, the profiles would have a parabolic shape, with a maximum in the middle, and a zero concentration at the edges, as observed in the case of high-temperature (70–105°C) testing [28]. This seems to indicate that, in the case under study, high-temperature exposure is not a good accelerated aging method.

The fact that the depth of the DOC penetration front tends toward a quasi asymptotic value $z_\infty$ at long time and that $z_\infty$ seems to be almost independent of aging conditions (in a relatively sharp temperature interval but with strong variations of the DOC concentration), can be explained on the basis of a simplified theory of diffusion controlled aging processes [29]. According to this theory, in the case where the mobile reactive species is consumed in a first-order process of rate constant $K$, the equilibrium depth $z_\infty$ of the reacted superficial layer is given by a simple scaling law as follows:

$$z_\infty = \left(\frac{D}{K}\right)^{1/2} \tag{12}$$

where $D$ is the diffusion coefficient of the reactive species.

It is noteworthy that $z_\infty$ is independent of the reactant concentration. Here, indeed, DOC is consumed by a second-order process as follows:

$$\mathrm{DOC} + \mathrm{PH} \rightarrow \text{products} \quad (k_{1S})$$

where PH is polyethylene.

The consumption of DOC by reactions with the antioxidant is negligible since this latter has disappeared in the superficial layer before the stabilization of the penetration front. The DOC consumption rate is thus given by the following:

$$\frac{d[\mathrm{DOC}]}{dt} = -k_{1S}[\mathrm{DOC}][\mathrm{PH}] \tag{13}$$

However, PH is slowly consumed so that, in the conversion range of practical interest:

$$[\mathrm{PH}] \approx [\mathrm{PH}]_0 = \text{constant} \tag{14}$$

The process appears thus as a pseudo-first-order process of rate constant:

$$K = k_{1S}[\mathrm{PH}] \tag{15}$$

Application of the above scaling law explains thus the invariance of the asymptotic depth of the DOC penetration front. Indeed, $z_\infty$ would probably undergo significant changes at temperatures very different from 20°C, because $D$ and $K$ have probably different activation energies.

Carbonyl profiles are considerably narrower than DOC penetration ones, as predicted by the model. Since, as seen in Part 1 of this article, chain scission is mainly due to oxidation processes, the molar mass profile is expected to have a shape similar to carbonyl one. No doubt, the cause of embrittlement and failure is situated in the relatively sharp oxidized layer of few hundred micrometers.

Let us now consider the primary function of the model, i.e., the prediction of time to failure $t_F$. The model seems to predict the good order of magnitude of $t_F$ in natural aging conditions, which is encouraging. Indeed, the prediction lacks of precision, first because local exposure conditions were known very approximately and were averaged to make a calculation in isothermal, isobaric conditions. Indeed, the question which comes in mind is as follows: Is it interesting to use a so sophisticated model only to appreciate orders of magnitude? It can be answered that: Since the model starts from a rate expression: $\dot{\varepsilon} = f(\sigma, T, t)$, it can work in nonisothermal, nonisobaric conditions provided that the stress $\sigma = f(t)$ and the temperature $T = g(t)$ variations are known. It is noteworthy that regression equations $\mathrm{Log}(\sigma) = f[\mathrm{Log}(t_F)]$ cannot offer this possibility. Thus, if, in a more or less remote future, local variations of temperature, pressure and DOC concentration are recorded, the precision on lifetime determination will be increased. Indeed, accelerated aging tries under pressure at constant temperature and DOC concentration would constitute a good validation way for the model. Unfortunately, they were not possible in the frame of this study. In the case where the local recording of exposure conditions would be economically impossible, it can be envisaged to complete this model, which is fully deterministic, by a probabilistic unit built from the statistical analysis of natural aging results. Such tools have been developed in other contexts and could be adapted to the case under study.

This model is not only a lifetime prediction tool, it can be also used to predict the trends of influence of the numerous operating parameters. Let us, for instance, consider the effect of antioxidant: The model predicts that it is practically inoperative because it is too fastly consumed by reactions with DOC to play a significant influence on polymer oxidation. In the region where DOC penetrates, DOC-PE reactions play the predominant role in the initiation of oxidation radical chains. This case of "extrinsic initiation" is not very different of the case of radiochemical aging where, also, the low-stabilizing efficiency of phenolic stabilizers has been put in evidence [30].

## CONCLUSIONS

A kinetic model aimed to predict the time to failure of PE pipes transporting drinking water disinfected by chlorine dioxide has been made. It is composed of two units as follows:

A chemical unit in which radical processes induced by DOC and oxygen are taken into account. Reaction-diffusion coupling is simulated to predict thickness concentration profiles of reactive species and reaction products. Three diffusing reactive species are considered as follows: DOC, oxygen, and the phenolic antioxidant. The main function of the model is to predict the molar mass $M_W$ value in the superficial layer at the polymer/water interface, because its decrease is the cause of embrittlement.

The mechanical unit is based on an empirical creep equation associated to a failure criterion. The creep rate depends essentially of time, temperature, and pressure. The failure criterion depends on weight average molar mass, which is given by the chemical unit.

The model parameters were identified from accelerated aging tests made at high DOC concentrations at 20 and 40°C on unloaded samples, and from natural aging tests on loaded samples. The model predicts the good order of magnitude for the time to failure in natural aging conditions. Its precision is very limited owing to the incertitudes on local aging parameters (temperature, pressure, DOC concentration). But, the model predicts satisfyingly certain trends, relative fort instance to antioxidant or carbonyl concentration profiles or to the lack of influence of antioxidants. It is thus not only a prediction tool but also an analysis tool allowing to express the influence of the numerous operative parameters into a mathematical form. It appears that DOC, which is a radical in ground state, is reactive with phenolic antioxidants and with polyethylene. It is able to initiate oxidation radical processes leading to chain scission. This latter is responsible for polymer embrittlement and premature failure. In natural aging conditions (temperature $\approx$ 15°C, DOC concentration $\approx$ 0.15 ppm, hoop stress of few MPa), lifetimes can be of the order of 10 years, sometimes shorter, against 50 years expected value.

## APPENDIX: CHEMICAL KINETIC MODEL

Since the chemical kinetic model must simulate thickness concentration profiles, diffusion-reaction coupling must be taken into account for the three molecular reac-

 DOI 10.1002/pen

tive species: oxygen, disinfectant, and stabilizer. That leads to the following equations:

$$\frac{d[O_2]}{dt} = D_{O2}\frac{\partial^2[O_2]}{\partial z^2} - k_2[O_2][P^\bullet] + k_{6a}[PO_2^\bullet]^2 \quad \text{(A-1)}$$

$$\frac{d[DOC]}{dt} = D_{DOC}\frac{\partial^2[DOC]}{\partial z^2} - k_{1d}[DOC][PH] - n_{AH}k_{1S}[DOC][AH] - k_7[DOC][P^\bullet] \quad \text{(A-2)}$$

$$\frac{d[AH]}{dt} = D_{AH}\frac{\partial^2[AH]}{\partial z^2} - n_{AH}k_{1S}[DOC][AH] - n_{AH}k_{S1}[PO_2^\bullet][AH] \quad \text{(A-3)}$$

where $n_{AH}$ is the phenolic stabilizer functionality.

The differential equation relative to $PO_2^\bullet$ radical becomes the following:

$$\frac{d[PO_2^\bullet]}{dt} = k_{1b}[POOH]^2 + k_2[O_2][P^\bullet] - k_3[PH][PO_2^\bullet] - k_5[P^\bullet]PO_2^\bullet] - 2k_{6a}[PO_2^\bullet]^2 - n_{AH}k_{S1}[PO_2^\bullet][AH] \quad \text{(A-4)}$$

All the other equations remain unchanged compared with the Part 1 of this article [1]. They are recalled here as follows:

$$\frac{d[P^\bullet]}{dt} = 2k_{1u}[POOH] + k_{1b}[POOH]^2 + k_{1d}[DOC][PH] - k_2[O_2][P^\bullet] + k_3[PH][PO_2^\bullet] - 2k_4[P^\bullet]^2 - k_5[P^\bullet][PO_2^\bullet] + 2k_{6d}[Q] - k_7[P^\bullet][DOC] \quad \text{(A-5)}$$

$$\frac{d[POOH]}{dt} = -k_{1u}[POOH] - 2k_{1b}[POOH]^2 + k_3[PH][PO_2^\bullet] + (1-\gamma_5)k_5[P^\bullet][PO_2^\bullet] \quad \text{(A-6)}$$

$$\frac{d[Q]}{dt} = k_{6a}[PO_2^\bullet]^2 - (k_{6b}+k_{6c}+k_{6d})[Q] \quad \text{(A-7)}$$

(Q = caged pair of $PO^\bullet$ radicals)

$$\frac{d[PH]}{dt} = -(2+\gamma_{1S})k_{1u}[POOH] - (1+\gamma_{1S})k_{1b}[POOH]^2 - k_{1d}[DOC][PH] - k_3[PH][PO_2^\bullet] + 2\gamma_4k_4[P^\bullet]^2 + (3\gamma_5-1)k_5[P^\bullet][PO_2^\bullet] + 2k_{6b}[Q] - 2(1+\gamma_{1S})k_{6d}[Q] \quad \text{(A-8)}$$

$$\frac{d[CO]}{dt} = \gamma_{1CO}k_{1u}[POOH] + \gamma_{1CO}k_{1b}\,[POOH]^2 + k_{6c}[Q] + 2\gamma_{1CO}k_{6d}\,[Q] \quad \text{(A-9)}$$

$$\frac{d[PCl]}{dt} = k_7[P^\bullet][DOC] \quad \text{(A-10)}$$

$$\frac{ds}{dt} = \gamma_{1S}k_{1u}[POOH] + \gamma_{1S}k_{1b}\,[POOH]^2 + 2\gamma_{1S}k_{6d}\,[Q] \quad \text{(A-11)}$$

$$\frac{dx}{dt} = \gamma_4k_4[P^\bullet]^2 + \gamma_5k_5[P^\bullet][PO_2^\bullet] + k_{6b}\,[Q] \quad \text{(A-12)}$$

$$\frac{1}{M_W} - \frac{1}{M_{W0}} = \frac{s}{2} - 2x \quad \text{(A-13)}$$

where $\gamma_{1S}$ and $\gamma_{1CO}$ are the respective yields of chain scissions and carbonyls from an alkoxy radical in the considered reactions (i.e., Iu, Ib, and VId).

## REFERENCES


1. X. Colin, L. Audouin, J. Verdu, M. Rozental-Evesque, B. Rabaud, and F. Martin, *Polym. Eng. Sci.* (in press).
2. N. Khelidj, X. Colin, L. Audouin, J. Verdu, C. Monchy-Leroy, and V. Prunier, *Polym. Degrad. Stab.*, **91**, 1593 (2006).
3. N. Khelidj, X. Colin, L. Audouin, and J. Verdu, *Nucl. Instrum. Methods Phys. Res. Sect. B*, **236**, 94 (2005).
4. J. Verdu, *J. Macromol. Sci. Pure Appl. Chem.*, **A3**, 1383 (1994).
5. X. Lu and N. Brown, *J. Mater. Sci.*, **25**, 29 (1990).
6. C.J.G. Plummer, "Microdeformation and Fracture in Semicrystalline Polymers," in *Mechanical Properties of Polymers Based on Nanostructure and Morphology*, G.H. Michler and F.J. Balta Calleja, Eds., Taylor and Francis, Boca Raton, Chap. 6, 216 (2005).
7. J. Viebke, E. Elble, M. Ifwarson, and U.W. Gedde, *Polym. Eng. Sci.*, **34**, 1354 (1994).
8. C. Munier, E. Gaillard-Devaux, A. Tcharktchi, and J. Verdu, *J. Mater. Sci.*, **37**, 4159 (2002).
9. H. Zweifel, *Plastics Additives Handbook*, *5th ed.*, Hanser Publishers, Munich, 10 (2001).
10. J. Viebke and U.W. Gedde, *Polym. Eng. Sci.*, **37**, 896 (1997).
11. J.B. Howard, *Polym. Eng. Sci.*, **13**, 429 (1973).
12. U.W. Gedde, J. Viebke, H. Leijstrom, and M. Ifwarson, *Polym. Eng. Sci.*, **34**, 1773 (1994).
13. J. Viebke, M. Hedvenquist, and U.W. Gedde, *Polym. Eng. Sci.*, **36**, 2896 (1996).
14. A. Lustiger, and R.L. Markham, *Polymer* **24**, 1647 (1983).
15. Y.L. Huan and N. Brown, *J. Polym. Sci. Part B: Polym. Phys.*, **29**, 129 (1991).
16. N. Brown, X. Lu, Y.L. Huang, and I. Qran, *Makromol. Chem. Makromol. Symp.*, **41**, 55 (1991).
17. R. Seguela, *J. Polym. Sci. Part B: Polym. Phys.*, **43**, 1729 (2005).
18. P.G. De Gennes, *J. Chem. Phys.*, **55**, 572 (1971).
19. B. Fayolle, X. Colin, L. Audouin, and J. Verdu, *Polym. Degrad. Stab.*, **92**, 231 (2007).
20. G.E. Schoolenberg, *J. Mater. Sci.*, **23**, 1580 (1988).
21. L. Audouin and J. Verdu, in *Radiation Effects on Polymers*, R.L. Clough and S.W. Shalaby, Eds., ACS Symposium

Series **475**, American Chemical Society, Washington, DC, 473 (1991).

22. S. Plantet, X. Colin, P. Chinesta, and G. Coffignal, Proceedings of CFM'07, Domaine Universitaire de St Martin d'Hères et de Gières, Grenoble, France, August 27–31 (2007).
23. A.S. Michaels and H.J. Bixler, *J. Polym. Sci*., **50**, 393 (1961).
24. J.Y. Moisan, *Eur. Polym. J*., **16**, 979 (1980).
25. X. Colin, L. Audouin, and J. Verdu, *Polym. Degrad. Stab*., **86**, 309 (2004).
26. N.C. Billingham and P.D. Calvert, in *Development in Polymer Stabilization*, G. Scott, Ed., Applied Science Publishers, Londres, 139 (1980).
27. P.D. Calvert and N.C. Billingham, *J. Appl. Polym. Sci*., **24**, 357 (1979).
28. J. Hassinen, M. Lundback, M. Ifwarson, and U.W. Gedde, *Polym. Degrad. Stab*., **84**, 261 (2000).
29. L. Audouin, V. Langlois, J. Verdu, and J.C.M. De Bruijn, *J. Mater. Sci*., **29**, 569 (1994).
30. A. Rivaton, S. Cambon, and J.L. Gardette, *Polym. Degrad. Stab*., **91**, 136 (2006).

 DOI 10.1002/pen